Journal of Systems Engineering and Electronics
Vol. 33, No. 2, April 2022, pp.340 – 344

Digital Earth surface maps for radar ground clutter simulation

ORESHKINA Margarita*, STEPANOV Maksim, and KISELEV Alexey

Novosibirsk State Technical University, Novosibirsk 630073, Russia

Abstract: This paper dwells upon optimizing the azimuth sampling interval of digital surface maps used to model radar ground clutter. The resulting equations can be used to find the digital map sampling interval for the required calculation error and modeled power of the simulated signal, which determines the resulting distribution of backscatter intensity. The paper further showcases how the sampling interval could be increased by preprocessing the map.

Keywords: ground clutter, mathematical modelling, radar, simulation.

DOI: 10.23919/JSEE.2022.000035

1. Introduction

Mathematical and semi-natural modeling of ground clutter uses digital vector-based surface maps as source data [1−5]. Traditionally [1−4], when describing the ground surface, several categories of its covers are classified (grass, forests, residential buildings, snow, and so on), each of which has its certain echoing properties set by the dependence of the normalized radar cross-section (nRCS) on the grazing angles. The location of the areas occupied by these cover and their configuration is identified by the map [1−4]. However, the vector format is inconvenient for the formation of the reflected signal, therefore discrete sampling is used to represent the continuous distribution of covers and the resulting distribution of reflectivity. This inevitably results in errors in the simulated signal parameters [3–8], thus making the simulated distribution of backscatter intensity error-prone as well. Errors can be reduced by sampling at smaller intervals. However, too small an interval will increase the computational complexity.

Many works described a discrete surface model but did not raise the issue of choosing a discretization step [2−5,8]. In some works, the step is determined based on the accuracy of the selected map [1,4], however, the impact of this choice on the characteristics of the simulated signal is not evaluated. In [6], the influence of the sampling step in azimuth on the simulation accuracy was shown and a method for determining the sampling rate based on the statistical properties of surface reflections was proposed.

The goal hereof is to substantiate methods that could increase the sampling interval while staying within the required margin of error of backscatter modeling.

Since the discrete array is formed by polar grid centered at the radar [1], there are azimuth and range sampling of Earth surface maps. Notably, sampling interval optimization for the range is for the most part a resolved issue [9,10]. This is why this paper focuses mainly on azimuth sampling.

Let us find out how the azimuth sampling interval affects the power of the simulated return of a pulse surveillance radar when scanning in the azimuth plane. As known [4,8,11], the distribution of reflectivity across the Earth's surface, i.e., the distribution of nRCS values at the points α for azimuth and r for slant range, which defines its radar image, can be represented by a random two-dimensional (2D) field. This field is denoted as $\sigma(\alpha, r)$. This distribution is weighted by the radiation patterns of the radar transmitter/receiver antennas, generating the antenna output and determining its power. As the power changes while the antenna system runs azimuth scanning, this change determines the Earth's surface radar image scanned by azimuth.

For azimuth scanning of the radiation pattern [8,12,13], the power of surface plots equidistant from the antenna (this distance is denoted as r) can be found as

$$P(\alpha_0, r) \sim \int_0^{2\pi} F(\alpha - \alpha_0, \theta(r) - \theta_0)\sigma(\alpha, r)\mathrm{d}\alpha \qquad (1)$$

where $F(\alpha, \theta)$ is the squared product of the pattern of transmitter and receiver antennas in the direction α and θ, α_0 and θ_0 are the pattern axis positions by azimuth and range, respectively, $\theta(r)$ is the elevation angle.

When using a discrete Earth surface map:

Manuscript received February 19, 2021.
*Corresponding author.
This work was supported by the Russian Foundation for Basic Research (19-37-90103).

$$P_d(\alpha_0, r) \sim S_{\text{es}} \cdot \sum_{i=1}^{N} F(i\Delta\alpha - \alpha_0, \theta(r) - \theta_0)\sigma(i\Delta\alpha, r) \quad (2)$$

where $\Delta\alpha$ is the azimuth sampling interval, S_{es} is the elementary cell area on the discrete map, N is the number of azimuthal nRCS distribution samples.

The difference between (1) and (2) is the error of the modeled clutter power, which arises from the sampling of surface reflectivity

$$E(\alpha_0, r) = P(\alpha_0,\ r) - P_d(\alpha_0,\ r). \quad (3)$$

Equations (1)–(3) can be used to find the errors of power of the modeled surface return from the given nRCS distribution and the radar pattern shape for a given nRCS azimuth sampling interval [6]. Let us now consider how to increase this interval.

2. Diminution the sampling interval requirements by using less detailed reflectivity specification

Let us use a known nRCS model [4,11], which can be expressed as

$$\sigma(\alpha, r) = \sigma_{0\_m}(\alpha, r) + \sigma_{0\_r}(\alpha, r) \quad (4)$$

where σ_{0_m} is a non-fluctuating component that depends on the cover type, σ_{0_r} is a random component that is a normal random process with the correlation function [14,15], which can be expressed as

$$R(\Delta_1, \Delta_2) = D_0 \exp\left(\frac{-\Delta_1 - \Delta_2}{\rho}\right) \quad (5)$$

where D_0 is the variance of the random nRCS component, ρ is the correlation radius, $\Delta_1 = a - b$ and $\Delta_2 = c - d$ are the distances between points on the axes α and r, a and b are the azimuth coordinates (α), c and d are the range coordinates (r).

In essence, σ_{0_r} forms a fine structure of nRCS distribution, which determines the sampling interval requirements. The question is when it does not have to be modeled.

Let us take a look at model (4) and find the equation of random and non-fluctuating RCS components for a plot of the Earth's surface sized $\Delta\alpha_L$ by Δr linearly. The linear size of such a plot in terms of the azimuth coordinate is related to the angular size ($\Delta\alpha$) by the following equation:

$$\Delta\alpha_L = \tan(\Delta\alpha) r.$$

The variance of the non-fluctuating RCS component [16] is defined as

$$D_m(\Delta\alpha, \Delta r) \sim \Delta\alpha_L^2 \Delta r^2 \sigma_{0\_m}^2. \quad (6)$$

The variance of the random RCS component in light of (5) is defined as

$$D_r(\Delta\alpha_L, \Delta r) \sim$$
$$\mathrm{D}\left[\int_0^{\Delta\alpha_L}\int_0^{\Delta r} \sigma_{0\_r}(\alpha, r)\partial r \partial\alpha\right] \sim$$
$$\int_0^{\Delta\alpha_L}\int_0^{\Delta\alpha_L}\int_0^{\Delta r}\int_0^{\Delta r} R(\Delta_1, \Delta_2)\partial a \partial b \partial c \partial d \sim$$
$$D_0 \int_0^{\Delta\alpha_L}\int_0^{\Delta\alpha_L} \exp\left(-\frac{|\Delta_1|}{\rho}\right)\partial a \partial b \cdot \int_0^{\Delta r}\int_0^{\Delta r} \exp\left(-\frac{|\Delta_2|}{\rho}\right)\partial c \partial d \quad (7)$$

where $\mathrm{D}[\cdot]$ is the symbol of variance calculation and $R(\Delta_1, \Delta_2) = D_0 \exp\left(-\frac{|\Delta_1|}{\rho} - \frac{|\Delta_2|}{\rho}\right)$.

Given that the integrand is even, each of the double integrals in (7) can be transformed into

$$\int_0^{\Delta\alpha_L}\int_0^{\Delta\alpha_L} \exp\left(-\frac{|\Delta_1|}{\rho}\right)\partial a \partial b =$$
$$2\int_0^{\Delta\alpha_L}\int_0^{b} \exp\left(-\frac{\Delta_2}{\rho}\right)\partial a \partial b =$$
$$2\int_0^{\Delta\alpha_L} \exp\left(\frac{b}{\rho}\right)\int_0^{b} \exp\left(-\frac{a}{\rho}\right)\partial a \partial b =$$
$$2\rho\left(\Delta\alpha_L + \rho \exp\left(\frac{-\Delta\alpha_L}{\rho}\right) - \rho\right).$$

Given that, the variance of the random RCS component will be written as

$$D_r(\Delta\alpha_L, \Delta r) \sim$$
$$4D_0\rho^2\left(\Delta\alpha_L - \rho + \rho\exp\left(\frac{-\Delta\alpha_L}{\rho}\right)\right)\cdot$$
$$\left(\Delta r - \rho + \rho\exp\left(\frac{-\Delta r}{\rho}\right)\right).$$

Thus, the variance equation can be expressed as

$$Y = \frac{D_r(\Delta\alpha_L, \Delta r)}{D_m(\Delta\alpha_L, \Delta r) + D_r(\Delta\alpha_L, \Delta r)}. \quad (8)$$

To illustrate this, consider modeling backscatter from a square grass-covered plot given the 3 cm operating radar wavelength with a grazing angle of six degrees. According to [11,17], in this case, $\sigma_{0\_m} = 10^{-3}$, $D_0 = 10^{-8}$, $\rho = 12$ m. Calculations run according to (8) show that the effect of the random component attenuates as the plot increases in size. For instance, for a 20 m × 20 m site, Y is approximately 4%; for an 80 m × 80 m site, Y is less than 1.5%.

3. Redacting the sampling rate by converting the original map

It is easy to see that (1) is a convolution of the nRCS distribution and the product of the antenna pattern. In turn,

(2) is a convolution of the discrete distribution of the nRCS and pattern. As for the frequency domain, transition to a discrete nRCS distribution results in its spectrum $G(f)$ being reproduced at an interval of $1/\Delta\alpha$. The spectrum of (2) is the nRCS spectrum $\hat{G}(f)$ multiplied by the spectrum of the product of the squared transmitter pattern and squared receiver pattern $F(\alpha,\theta)$, which is denoted as $G_F(f)$.

This periodic reproduction of the nRCS distribution spectrum value results in a well-known phenomenon referred to as spectral overlap, as shown in Fig. 1. If the spectral overlap occurs in a domain bounded by $G_F(f)$, the spectrum of (2) will differ from that of (1). Since $\sigma(\alpha,r)$ has an infinitely broad spectrum [12], overlap will occur at any sampling rate.

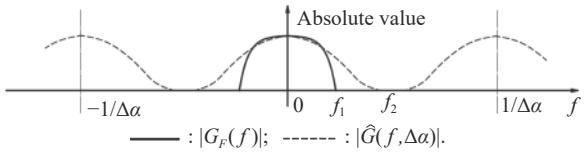

Fig. 1 Absolute values of the functions $G_F(f)$ and $\hat{G}(f)$

However, the functions $G_F(f)$ and $G(f)$ are monotonically decreasing [12], which enables finding such rates f_1 and f_2, respectively, above which the function values can be neglected (assumed to equal zero). Then, given that $G_F(f)$ and $G(f)$ must intercept at the given level, the sampling rate must be (see Fig. 1)

$$f_d \geqslant f_1 + f_2.$$

This equation allows lowering the sampling rate. It is essentially as follows. If $f_2 \leqslant f_1$, then filtering the nRCS distribution with a low-frequency filter whose bandwidth equals f_1 will return $f_d \geqslant 2f_1$.

This allows reducing the nRCS distribution sampling interval by a factor of

$$(f_1 + f_2)/2f_1. \tag{9}$$

The reduced sampling rate and the corresponding increase in the sampling interval will not lead to a greater error (see Fig. 1). In essence, the pattern shape and width determine the sampling interval. This leads to two important conclusions.

First, it is necessary to find the sampling rate f_1 for the typical approximations of the main pattern lobe: the Gaussian function, the 2nd- and the 3rd-degree cosine, and the sinc function. Table 1 summarizes the estimates for three values of the normalized level (denoted as ε). It shows the values f_1 depending on the main-lobe width for the first-zero level (denoted as W_{00}) (for half-power level in case of the Gaussian function W_{05}) and the number of discrete samples per equal range ring N.

Table 1 Necessary cover azimuth sampling rate for the most common pattern models

Antenna pattern approximation	The upper frequency of the spectrum f_1		
	$\varepsilon = 0.001$	$\varepsilon = 0.01$	$\varepsilon = 0.1$
$F(\alpha) = \exp\left(\frac{4\ln(0.5)}{W_{05}}\alpha^2\right)^2$	$2.8N/W_{N05}$	$2.3N/W_{N05}$	$1.7N/W_{N05}$
$F(\alpha) = \left(\frac{\sin(2\pi\alpha/W_{00})}{2\pi\alpha/W_{00}}\right)^2$	$3.8N/W_{N00}$	$3.4N/W_{N00}$	$2.6N/W_{N00}$
$F(\alpha) = \cos^2\left(\frac{\pi}{W_{00}}\alpha\right)$	$3.1N/W_{N00}$	$2.9N/W_{N00}$	$2.3NW_{N00}$
$F(\alpha) = \cos^3\left(\frac{\pi}{W_{00}}\alpha\right)$	$4N/W_{N00}$	$3.6N/W_{N00}$	$2.7N/W_{N00}$

Second, prefiltering the original nRCS distribution (the original vector-based map) by azimuth using a low-pass filter with a bandwidth of f_1 helps reduce the sampling rate of the original nRCS distribution to $2f_1$.

In general, these findings allow creating an algorithm that will calculate the sampling interval for digital nRCS distribution maps as follows:

(i) Use (8) to assess the need to model the random component. If such modeling is not needed, set this component to 0.

(ii) Filtering the original nRCS distribution (the original vector-based map) by azimuth using a low-pass filter with a bandwidth of f_1.

(iii) Set the sampling interval according to $f_d \geqslant 2f_1$.

4. Experiments

Example 1 Let us consider the modeling of a 10 km radius ground surface area, whose distribution of RCS is shown in Fig. 2 (antenna mast height is 5 m). For this purpose, a threshold is chosen to determine the upper frequency of the spectrum-such a frequency, above which harmonics values do not exceed 0.1 of the maximum harmonic in spectrum.

Fig. 2 Ground clutter map

The original map of the area is split into 300 round ranges. Within each round, 10 000 samples of the nRCS are taken and the upper frequency is calculated based on them. Thus, we receive 300 frequency values (as shown in Fig. 3), and to calculate the required sampling frequency, we will select the maximum of them, which is 0.3.

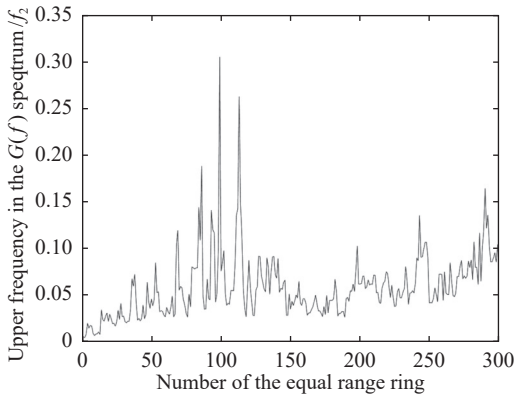

Fig. 3 Dependence of the frequency f_2 on the number of a ring of equal range for the distribution is shown in the Fig. 2 ($\varepsilon = 0.1$)

Let us choose a Gaussian function as an approximation of the antenna directivity diagram. To calculate the frequency f_1, we find the number of counts per beam width:

$$W_{05} = \frac{10\,000 \cdot W_{\text{deg}}}{360}$$

where W_{deg} is antenna beamwidth in degree.

Then, using the formula from Table 1, we calculate the value of the upper frequency f_1 of the antenna diagram of a Gaussian shape, with a width of 1, 2, and 3 degrees. The value of the frequency f_1 and the gain (9) are entered in Table 2.

Example 2 Let us consider the same surface area for a higher antenna position (antenna mast height is 25 m). The Fig. 4 presents this map (maximum range is 10 km, cells with discernible clutter are shown white, the map is calculated for the height of the antenna mast equal to 25 km). In this case, a larger number of surface areas are illuminated (as shown in Fig. 4) and the distribution of the nRCS is more uniform. This leads to a decrease of the upper frequency f_2 (as shown in Fig. 5). In this example, $f_2 = 0.045$. The gain (9) for this example is listed in Table 2.

Table 2 Dependence of the gain (9) on the antenna beamwidth

Antenna beamwidth in degree	Gain of the method		
	1/(°)	2/(°)	3/(°)
Frequency f_1 ($\varepsilon = 0.1$)	0.06	0.03	0.02
Gain (9) for the Example 1	3	5.5	8
Gain (9) for the Example 2	–	1.25	1.6

Fig. 4 Ground clutter map

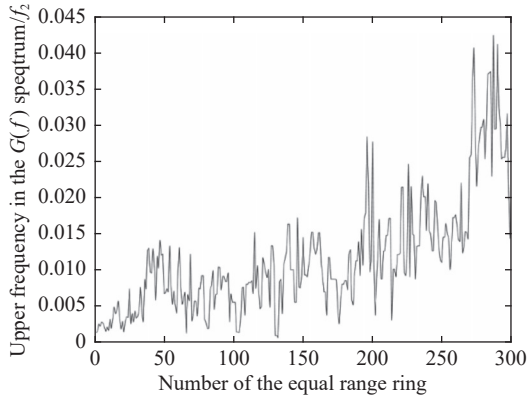

Fig. 5 Dependence of the frequency f_2 on the number of a ring of equal range for the distribution is shown in Fig. 4 ($\varepsilon = 0.1$)

Example 3 Let us consider the modeling of the section from Fig. 3. However, now the threshold for determining the upper frequency is 0.01. For this case, the frequency distribution is shown in Fig. 6. The upper fre-

quency can be taken as equal to 0.5. The frequencies f_1 for different beamwidth and the resulting gain are listed in Table 3.

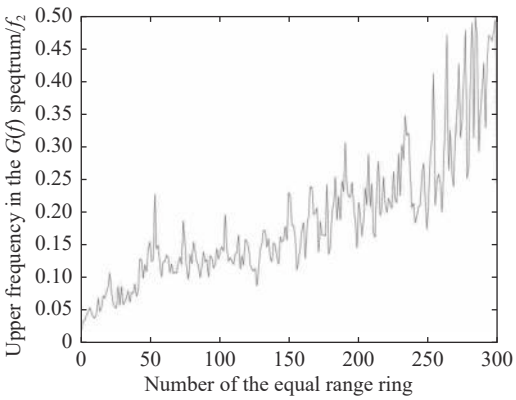

Fig. 6 Dependence of the frequency f_2 on the number of a ring of equal range for the distribution is shown in Fig. 4 ($\varepsilon = 0.01$)

Table 3 Dependence of the gain (9) on the antenna beamwidth

Antenna beamwidth in degree	Gain of the method		
	1/(°)	2/(°)	3/(°)
Frequency f_1 ($\varepsilon = 0.01$)	0.08	0.04	0.03
Gain (9) for the Example 2	3.6	6.7	8.8

As the examples show, this method is well suited for modeling highly irregular ground surfaces when there is a lot of shading. This is typical when the radar is operating at low grazing angles [1]. The method is also good for cases where it is necessary to carry out simulations with higher accuracy. At the same time, the method is more effective when simulating the operation of radars with wide antenna beams.

5. Conclusions

Equations obtained can be used to find the minimum allowed sampling interval for Earth surface maps given the required error of simulated signal power.

The paper shows how to reduce this interval by not modeling the random nRCS distribution component and by filtering the original distribution.

References

[1] BILLINGSLEY J B. Low-angle radar land clutter-measurement and empirical models. Norwich: William Andrew Publishing, 2002.
[2] FENG S S, CHEN J. Low-angle reflectivity modeling of land clutter. IEEE Geoscience and Remote Sensing Letters, 2006: 254–258.
[3] RYAN J S, SAVILLE M A, PARK J. Modeling terrain profiles from digital terrain elevation data and national land cover data. Proc. of the SPIE, 2016. DOI: 10.1117/12.2225338.
[4] KULEMIN G P. Millimeter-wave radar targets and clutter. Boston: Artech House, 2003.
[5] GRECO M S, WATTS S. Academic press library in signal processing. New York: Academic Press, 2014.
[6] ORESHKINA M V, KISELEV A V. On the errors arising from the use of discrete surface models for land clutter simulation. Proc. of the XIV International Scientific-Technical Conference on Actual Problems of Electronic Instrument Engineering, 2018.
[7] RICHARDS M A, SCHEER J A, HOLM W A. Principles of modern radar: basic principles. Edison: Scitech Publishing, 2010.
[8] NATANSON F E, REILLY J P, COHEN M N. Radar design principles: signal processing and the environment. Edison: Scitech Publishing, 2004.
[9] BELORUTSKY R Y, NIKULIN A V. The substitution of earth surface by discrete model when imitating echo signal reflected from it. Issues of Radio Electronics, 2012, 4: 134–144.
[10] ORESHKINA M V, KISELEV A V. Discrete model of earth reflectivity for land clutter simulation. Proc. of the International Multi-conference on Engineering, Computer and Information Sciences, 2019: 639–640.
[11] KULEMIN G P, GOROSHKO E A, TARNAVSKY E V. Spatio-temporal characteristics of backscatters from the earth serface. Success in Modern Electronics, 2004, 12: 60–70. (in Russian)
[12] SKOLNIK M I. Radar handbook. 3rd ed. New York: McGrew-Hill, 2008.
[13] TVERSKOY G N, TERENTYEV G N, KHARCHENKO I P. Echo simulators for marine radar. Leningrad: Sydostroenie, 1973. (in Russian)
[14] DARAWANKUL A, JONSON J T. Band-limited exponential correlation function for rough-surface scattering. IEEE Trans. on Geoscience and Remote Sensing, 2007, 45(5): 1198-1206.
[15] HABIBI A. Two dimensional Bayesian estimate of image. Proceedings of the IEEE, 1972, 60(7): 878–883.
[16] GAUR Y N, SRIVASTAVA N. Statistics and probability theory. 7th ed. Jaipur: Genius Publications, 2013.
[17] BILLINGSLEY J B, FARINA A, GINI F, et al. Statistical analyses of measured radar ground clutter data. IEEE Trans. on Aerospace and Electronic Systems, 1999, 35(2): 579–593.

Biographies

ORESHKINA Margarita was born in 1991. She received her M.S. degree in radioengineering in 2017. She is a lecturer in Novosibirsk State Technical University. Her current research interests include modeling of radar echo signals and mathematical modeling.
E-mail: oreskina.m@yandex.ru

STEPANOV Maksim was born in 1982. He is a Ph.D. of technical sciences and professor of the Department of Radio Receivers and Radio Transmitters, Novosibirsk State Technical University. His current research interests include design of mathematical models of radar echo and simulators of radar situations and real-time simulation of complex radar conditions.
E-mail: m.stepanov@corp.nstu.ru

KISELEV Alexey was born in 1958. He is a Ph.D. of technical sciences and professor of the Department of Radio Receivers and Radio Transmitters, Novosibirsk State Technical University. His current research interests include real-time modeling of a complex radar environment, radar clutter simulation, and mathematical modeling.
E-mail: a.kiselev@corp.nstu.ru